LIMNOLOGY and OCEANOGRAPHY

ASLO

Limnol. Oceanogr. 66, 2021, 1896–1914

doi: 10.1002/lno.11731

Seasonal shifts of microbial methane oxidation in Arctic shelf waters above gas seeps

Friederike Gründger,[1,2*] **David Probandt**,[3] **Katrin Knittel**,[3] **Vincent Carrier**,[1,4] **Dimitri Kalenitchenko**,[1] **Anna Silyakova**,[1] **Pavel Serov**,[1] **Bénédicte Ferré**,[1] **Mette M. Svenning**,[1,4] **Helge Niemann**[5,6,1]

[1]CAGE—Centre for Arctic Gas Hydrate, Environment and Climate, Department of Geosciences, UiT The Arctic University of Norway, Tromsø, Norway
[2]Arctic Research Centre, Department of Biology, Aarhus University, Aarhus, Denmark
[3]Department of Molecular Ecology, Max Planck Institute for Marine Microbiology, Bremen, Germany
[4]Department of Arctic and Marine Biology, UiT The Arctic University of Norway, Tromsø, Norway
[5]Department of Marine Microbiology & Biogeochemistry, NIOZ Royal Netherlands Institute for Sea Research, Texel, The Netherlands
[6]Department of Earth Sciences, Faculty of Geosciences, Utrecht University, Utrecht, The Netherlands

Abstract

The Arctic Ocean subseabed holds vast reservoirs of the potent greenhouse gas methane (CH_4), often seeping into the ocean water column. In a continuously warming ocean as a result of climate change an increase of CH_4 seepage from the seabed is hypothesized. Today, CH_4 is largely retained in the water column due to the activity of methane-oxidizing bacteria (MOB) that thrive there. Predicted future oceanographic changes, bottom water warming and increasing CH_4 release may alter efficacy of this microbially mediated CH_4 sink. Here we investigate the composition and principle controls on abundance and activity of the MOB communities at the shallow continental shelf west of Svalbard, which is subject to strong seasonal changes in oceanographic conditions. Covering a large area (364 km^2), we measured vertical distribution of microbial methane oxidation (MOx) rates, MOB community composition, dissolved CH_4 concentrations, temperature and salinity four times throughout spring and summer during three consecutive years. Sequencing analyses of the *pmoA* gene revealed a small, relatively uniform community mainly composed of type-Ia methanotrophs (deep-sea 3 clade). We found highest MOx rates (7 nM d^{-1}) in summer in bathymetric depressions filled with stagnant Atlantic Water containing moderate concentrations of dissolved CH_4 (< 100 nM). MOx rates in these depressions during spring were much lower (< 0.5 nM d^{-1}) due to lower temperatures and mixing of Transformed Atlantic Water flushing MOB with the Atlantic Water out of the depressions. Our results show that MOB and MOx in CH_4-rich bottom waters are highly affected by geomorphology and seasonal conditions.

Temperature rise in the Arctic and its impact on the environment is more severe than for any other region on Earth (Masson-Delmotte et al. 2006; Hansen et al. 2013). The Arctic Ocean holds vast reservoirs of CH_4, which has a 32-fold higher greenhouse warming potential than carbon dioxide and may be released into the ocean and the atmosphere (Etminan et al. 2016). The majority of the CH_4 reservoirs across the Arctic shelves are temperature-sensitive, e.g., subsea permafrost (Shakhova et al. 2010) and gas hydrates in shallow sediments (Westbrook et al. 2009; Berndt et al. 2014). Gaseous CH_4 released from the seafloor becomes dissolved and can then be utilized by aerobic methane-oxidizing bacteria (MOB), which use CH_4 as an energy source and carbon substrate for growth (e.g., Hanson and Hanson 1996; Murrell 2010). In the ocean, aerobic microbial methane oxidation (MOx) is the final sink for

*Correspondence: friederike.gruendger@bio.au.dk

Additional Supporting Information may be found in the online version of this article.

Author Contribution Statement: F.G. and H.N. designed the project. F.G., H.N., V.C. collected the samples, carried out the main experiments. A.S. provided and analyzed hydrographic data. D.P., D.K., V.C., and K.K. carried out bioinformatic and quantification analyses. P.S. analyzed CH_4 concentrations. M.S. and H.N. supervised the research and contributed with scientific discussions. F.G. carried out interpretation of the experiments and wrote the manuscript with contribution from all co-authors.

CH_4 before it is liberated to the atmosphere (Reeburgh 2007), but little is known about the diversity, abundance, distribution, and activity of MOB (Tavormina et al. 2008; Mau et al. 2013; Steinle et al. 2015). For example, high amounts of CH_4 were rapidly consumed by MOB following the deep-water horizon accident (Crespo-Medina et al. 2014) and MOB were found to effectively consume CH_4 from the water column if hydrographic conditions provide continuity for MOB (Steinle et al. 2015, 2017). However, MOx can also be very low despite high CH_4 concentrations in marine waters for reasons that are still unclear (Bussmann 2013).

Aerobic MOB are phylogenetically divided into Gammaproteobacteria (type I MOB), Alphaproteobacteria (type II MOB) (e.g., Hanson and Hanson 1996; Knief 2015), and Verrucomicrobia (type III MOB) (Dunfield et al. 2007; Op den Camp et al. 2009; van Teeseling et al. 2014). Common to almost all MOB is the presence of the membrane-bound particulate methane monooxygenase, the enzyme responsible for the initial step of methane oxidation. The highly conserved *pmoA* gene, encoding a subunit of the particulate methane monooxygenase, is most frequently used as a molecular marker both for detection and phylogeny of MOB via cultivation-independent methods (Tavormina et al. 2008; Knief 2015). Potential methane-oxidizing uncultivated clades like the deep-sea clades 1–5 (Lüke and Frenzel 2011) have been identified by this approach. Especially in marine environments, great uncertainties exist about the factors that determine MOB activity and community structure. From the Arctic marine environment, a number of studies report on MOx activity and MOB community composition in relation to environmental factors such as CH_4 concentrations and hydrography (e.g., Mau et al. 2013; Steinle et al. 2015; Osudar et al. 2016). However, all those studies are single snap-shots of the prevailing situation at the place and time of sampling. For example, studies focusing

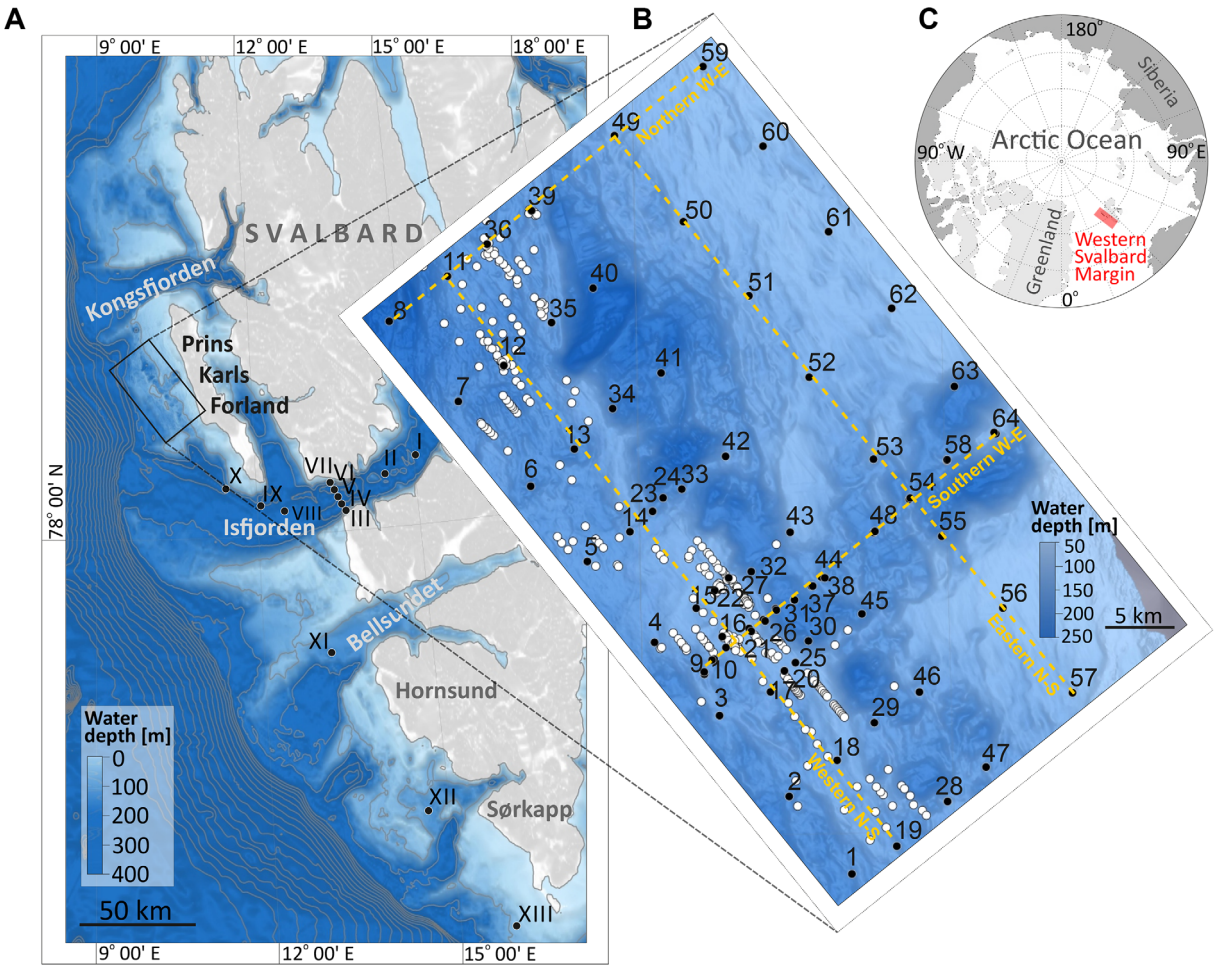

Fig 1. Bathymetric map of the study areas west off Svalbard archipelago showing hydrographic sampling stations indicated by black dots at Isfjorden (Stas. I–X), Outer Bellsundet (Sta. XI), Outer Hornsund (Sta. XII), and Sørkappøya (Sta. XIII) (**A**). Detailed map of the shallow shelf west of Prins Karls Forland including gas flare locations (white dots) and 64 sampling stations arranged in a grid. At stations along the four transects (conducted from North to South and West to East, yellow dashed lines), sampling for methane oxidation rates and microbial molecular analyses were conducted in addition to hydrographic profiles and CH_4 concentrations, which were usually conducted at all stations (**B**). Global view of our sampling area at the western Svalbard margin (**C**).

on areas around the Svalbard archipelago, i.e., the continental slope west of Prins Karls Forland (Gentz et al. 2014), Storfjorden in the south-east (Mau et al. 2013), and the Svalbard margin between Bjørnøya and Kongsfjordrenna (south to west Svalbard) (Mau et al. 2017), were only conducted without temporal repetition in August/September. Only Steinle et al. (2015) compared spatiotemporal replicates collected during several surveys at the Svalbard continental margin in late August. Time series studies covering seasonal changes of CH_4 input and microbial CH_4 turnover in the water column in the Arctic have so far not been published, and little knowledge exists on the community composition of Arctic Ocean MOB (James et al. 2016; Ferré et al. 2020).

In this study, we investigate the fate of CH_4 in the water column at the continental margin west of Svalbard, specifically the shallow shelf west off Prins Karls Forland. This area is characterized by CH_4 seepage (Portnov et al. 2016; Silyakova et al. 2020). Despite extensive release of CH_4 from the sediment in this area, almost no CH_4 was found to reach the atmosphere (Myhre et al. 2016). Our main objectives were (1) to study the composition and activity of the methanotrophic communities, (2) to investigate seasonal shifts and, related to these, (3) the differential hydrographical settings and their influence on MOB activity and distribution within the study area. To meet these aims, we conducted sampling surveys in the spring, late spring and summer.

We found that community changes of MOB are marginal, but that MOx capacity is influenced by seasonal shifts and varies according to site-specific geographical features and changing hydrographical conditions.

Methods

Study area

Our study area stretches along the continental margin off western Svalbard from the shallow shelf west of Prins Karls Forland towards the southern tip of Svalbard including Isfjorden, Isfjorden Trough, Outer Bellsundet, Outer Hornsund, and Sørkappøya (Fig. 1). Water depth in these areas ranges from 50 to 160 m. The shallow shelf west of Prins Karls Forland is characterized by an irregular bathymetry showing numerous large depressions encompassed by a series of moraine ridges termed the Forlandet moraine complex (Landvik et al. 2005; Fig. 1B). Here, along the Forlandet moraine complex in 80–90 m water depth, a vast number of gas flares (~200 flares, identified by acoustic signatures of gas bubbles in the water) were previously mapped (Sahling et al. 2014; Silyakova et al. 2020). The $\delta^{13}C$ values of the emitted CH_4 and the absence of higher hydrocarbons in the seeping gas indicates a microbial CH_4 origin (Graves et al. 2017; Mau et al. 2017). The seepage region west of Prins Karls Forland lies > 200 m shallower than the upper limit of the methane hydrate stability zone and unlikely results from CH_4 hydrates dissociating in situ. However, lateral migration of CH_4 from a hypothesized gas hydrate dissociation front at deeper shelf settings may at least partly fuel the seeps on the shallow shelf (Sarkar et al. 2012).

The hydrodynamics in our study area are complex (see also Silyakova et al. 2020). The East Spitsbergen Current flows along the Svalbard islands southwards on the east side, following the coast around the island's southern tip and then turns northwards on the west side of the island (Nilsen et al. 2008). Here, it flows as a coastal current on the shelf and is composed of less saline and cold Arctic Water (34.30–34.80, −1.5 to 1.0°C) into our study area. To the west of the shelf, the northernmost extension of the North Atlantic Current, the West Spitsbergen Current (Aagaard et al. 1987) is composed of relatively saline and warm Atlantic Water (> 34.65, > 3.0°C) and also flows northward. Although the East Spitsbergen Current and West Spitsbergen Current are separated by a front, frequent mixing occurs and the West Spitsbergen Current may also flood the shelf (Steinle et al. 2015). Seasonality defines the different portions of mixed water masses. Atlantic Water transforms into Transformed Atlantic Water (> 34.65, 1.0–3.0°C) by losing heat to the atmosphere and adjacent waters and freshening due to meltwater from glaciers, snow and sea ice. Whereas Intermediate Water (34.00–34.65, > 1.0°C) is formed by entrainment and mixing mechanisms at the boundary of Surface Water with underlying Atlantic Water or Transformed Atlantic Water. Surface Waters are freshened by melt water and warmed by solar heat in summer (< 34.00, < 1.0°C). Waters that overwinter in fjords become colder and fresher, and are then classified as Local Water mass (34.30–34.85, −0.5 to 1.0°C). Water masses are classified according to Cottier et al. (2005).

Sampling strategy

Samples were taken within three successive years (2015–2017) during four expeditions with R/V *Helmer Hansen*,

Table 1. Sampling strategy and definitions of water samples/horizon taken from the water column.

Water depth	CH_4	MOx	16S rRNA	Water level	Water layer
5 m below sea surface	x	x	x	8	Surface
15 m below sea surface	x	x		7	
25 m below sea surface	x	x		6	
Intermediate 2	x	x	x	5	Intermediate
Intermediate 1	x	x		4	
25 m above seafloor	x	x	x	3	Bottom
15 m above seafloor	x	x		2	
5 m above seafloor	x	x	x	1	

CAGE16-4 (spring: 2–4 May 2016), CAGE17-1 (spring: 16–20 May 2017), CAGE16-5 (late spring: 17–22 June 2016), and CAGE15-3 (summer: 1–3 July 2015). At the shallow shelf west of Prins Karls Forland, we collected samples at 64 hydrographic stations arranged in a grid pattern covering an area of approximately 14 × 26 km. All stations were sampled successively (total sampling time of the entire grid < 72 h). The positions of transects and stations were selected according to their coverage of specific features found at the seafloor such as gas flares or bathymetric depressions (Fig. 1B). For example, the western N-S transect follows the main ridge of the Forlandet moraine complex and covers numerous CH_4 flares. The southern W-E transect features a flare cluster in the west and covers bathymetric depressions towards the east. During the June survey in 2016, time constrains allowed us to only sample 12 of the 64 stations. Those 12 stations were located along the western N-S, eastern N-S, and southern W-E transects (Fig. 1B, Table S1).

At all stations, hydrographic parameters (salinity, temperature, pressure) were recorded at 24 Hz with a Conductivity-temperature-depth profiler (SBE 911 plus CTD; Sea-Bird Electronics, Inc., USA) equipped with twelve 5-liter Teflon-lined Niskin bottles. Only downcasts were used for hydrographic profiling. With the CTD-mounted Niskin bottles, we collected discrete water samples from eight water levels (1–8): 5, 15, 25 m above seafloor, 5, 15, 25 m below sea level, and two additional intermediate sampling levels evenly spaced between 25 m below sea level and 25 m above seafloor (actual sampling depth depending on water depth; Table 1). Water from the Niskin bottles was subsampled immediately upon recovery. Dissolved CH_4 concentrations were measured in all eight water levels of the entire sampling grid. MOx rates were measured in all eight water levels along four transects, which run from north to south (eastern N-S and western N-S) and west to east (northern W-E and southern W-E) (comprising 31 stations, Fig. 1B). Samples for phylogenetic analyses were recovered during sampling campaigns in July 2015 as well as May and June 2016 (but not in May 2017) from water levels 1, 2, 3, 5, and 8 from all stations where MOx rates were measured. During the May 2016 campaign, six stations (Stas. 9, 16, 31, 44, 54, and 64) along the southern W-E transect were repeatedly investigated 2 days after the first sampling to monitor rapid variations of hydrographic conditions and their effects on MOx activity and bacterial community changes.

In addition to the shallow shelf west of Prins Karls Forland, in May and June 2016 we investigated the water column at Isfjorden (Stas. I and II), Isfjorden Trough (III–X), Outer Bellsundet (XI), Outer Hornsund (XII), and Sørkappøya (XIII) (Fig. 1A, Table S1) in the same manner as described above. CTD and dissolved CH_4 concentration data from the surveys in July 2015 and June 2016 of the area west of Prins Karls Forland were published by Silyakova et al. (2020).

Methane concentration measurements

Methane concentrations were determined using a headspace method as described by Silyakova et al. (2020). In order to calculate the content of dissolved CH_4 of the entire sampling area at the shallow shelf of Prins Karls Forland, we defined three water layers with consideration of the uneven bathymetry (Silyakova et al. 2020). Water layers were defined as the "Bottom Water Layer" from seafloor to 25 m above seafloor (comprising levels 1, 2, and 3), the "Surface Water Layer" from the ocean surface down to 25 m depth (comprising levels 8, 7, and 6), and the "Intermediate Layer" between 25 m below the ocean surface and 25 m above seafloor (comprising levels 5 and 4) (Table 1).

Methane oxidation rate measurements

Methane oxidation rates were determined according to previous publications (Niemann et al. 2015; Steinle et al. 2015) with modifications as described in Ferré et al. (2020). For the water column at the sampling area west of Prins Karls Forland, the mean areal turnover of CH_4 was calculated by integrating distinct MOx rates over depth yielding results in m^{-2} d^{-1} for each water layer and the entire water column (Steinle et al. 2017). We then calculated weighted MOx means for each layer, considering uneven horizontal spacing of the hydro cast stations (for a more detailed description of the computation of the weighted means see Silyakova et al. (2020)). Upscaled to the size of the sampling grid (423 km^2), these weighted means translate to a total CH_4 turnover per day for each water layer and the entire water body of the sampling grid. To compare the capacity of MOx to retain CH_4, we then calculated the fraction of CH_4 consumed per day:

$$CH_4\ \text{turnover per day}\ (\%) = MOx/CH_4 \times 100 \quad (1)$$

Bacterial community analyses

Seawater samples for molecular analysis were collected in sterile, high-density polyethylene bottles and usually processed immediately after subsampling. However, time constraints sometimes required storage of samples at 4°C in the dark before further processing, but storage time never exceed 4 h. We filtered a volume of 1 liter of sample on membrane filters (Whatman Nuclepore Track-Etched PC, 0.22 μm, Merck Millipore, MA) by applying a gentle vacuum of ~ 0.5 bar and stored filters at −20°C until further analyses. Total DNA from membrane filters was extracted following the method of Pilloni et al. (2012) and DNA content in each sample was quantified using a spectrophotometer (Nanodrop, ND-1000, Thermo Scientific, MA).

For the amplification of the bacterial 16S rRNA gene, we selected samples retrieved in July 2015, May 2016 and June 2016 from distinct water levels from Prins Karls Forland (Stas. 9, 10, 19, 49, 54, 58; levels 1, 3, 5, and 8), from Isfjorden (Sta.

I; levels 1 and 3) and Outer Bellsundet (Sta. XI; levels 2 and 4) (Table S1). We used the degenerated primer pair Bakt_341F and Bakt_805R resulting in about 450 bp amplicons covering the V3-4 region of the 16S rRNA gene (Herlemann et al. 2011). For the amplification of the particulate methane monooxygenase gene (*pmoA*), we selected samples from the abovementioned sampling campaigns from the water level 1 from Prins Karls Forland stations 9, 10, 49, 54, 58, and Isfjorden (Sta. I), and from water level 2 from Outer Bellsundet (Sta. XI). Water levels 1 and 2 were selected, because of elevated MOx rates, which were measured at these particular water levels at the chosen stations. The primer pair wcpmoA189f and wcpmoA661r for marine water column MOB (Tavormina et al. 2008) was used for amplification. Gene analyses of 16S rRNA and *pmoA* amplicons were performed by IMGM Laboratories GmbH (Martinsried, Germany). Cluster generation and bidirectional sequencing (2×300 nt) by synthesis was accomplished on the Illumina MiSeq next generation sequencing platform (Illumina, CA) using reagents kit 500 cycles v2 under the control of MiSeq Control Software v2.5.1.3. Sequence data have been submitted to the GenBank Sequence Read Archives (https://www.ncbi.nlm.nih.gov/sra) under BioProject ID: PRJNA642858 (16S rRNA) and PRJNA641979 (*pmoA*).

Processing of 16S rRNA gene sequences was achieved as outlined in the following. Using BBMerge software version 37.02 (BBTools package, Brian Bushnell, Walnut Creek, CA), we performed the initial data processing of the raw sequences (primer trimming, quality filtering at a minimum of 99.1% base call accuracy, and read assembly of forward and reverse read with an overlap of 20 bp by default strictness setting). The resulting reads were processed according to the MiSeq standard operating procedure (Kozich et al. 2013) with MOTHUR version 1.39.5 (Schloss et al. 2009) including pre-clustering at 99% sequence similarity and de novo-based chimera removal using UCHIME (Edgar et al. 2011) to remove artificial diversity. Sequences were aligned and classified using the SILVA reference database (Release 132; Quast et al. 2013). Sequences classified as "no relative," chloroplast, archaeal and eukaryotic 16S rRNA were removed. Afterwards, bacterial sequences were clustered into operational taxonomic units (OTUs) at 97% sequence similarity, using the OptiClust algorithm. To reduce artificial diversity, rare $OTU_{0.97}$ that were represented by only ≤ 2 sequences in the whole dataset were removed as suggested for short fragment 16S rRNA gene data (Allen et al. 2016). Prior to diversity analysis, OTUs retrieved for the blank DNA extraction and the no template negative control from the library preparation were also removed from the entire data set.

After MOTHUR sequence processing and prior to statistical and diversity analysis, the community dataset was randomly rarified to the lowest number of sequences found per sample (1083). We conducted alpha and beta diversity analyses using the program R with the vegan package (v. 2.5-6; https://CRAN.R-project.org/package=vegan). Displaced alpha diversity values are the means of 25 iterations. Hierarchical clustering and Non-Metric Multidimensional Scaling (NMDS) analyses are based on the Bray–Curtis dissimilarity index. Spearman's rank correlation of bacterial phyla at the family level and selected environmental variables was conducted with R package Hmisc (v.4.4-0; https://CRAN.R-project.org/package=Hmisc). Only those family level clades (SILVA taxonomy v.132) that contributed $\geq 0.5\%$ to total sequences in at least one sample were considered.

We processed *pmoA* amplicons as follows: The raw sequences were treated following our open-access pipeline (https://github.com/dimikalen/MS_UIT_CAGE/blob/master/CAGE_MiSeq_SOP.sh). Briefly, forward and reverse reads were merged using BBmerge (v37.36; Bushnell et al. 2017) and quality filtered with a maxEE parameter of 1 in VSEARCH (v2.9.0; Rognes et al. (2016)). To reduce the computational need in the following steps, unique sequences were extracted. Operational phylogenetic units (OPUs) were defined by using USEARCH (v11; Edgar (2010)) applying a similarity threshold of 97%. The most abundant reads of each OPU were then selected to find the closest known sequences in the *pmoA* gene reference database (on nucleotide level, Wen et al. (2016)) using the Wang method in MOTHUR (v1.39; Schloss et al. 2009). All raw *pmoA* reads were then mapped back to the reference reads of the *pmoA* $OPU_{0.97}$, as recommended in the USEARCH documentation, in order to construct the final OPU table. The OPU table was subsequently rarefied at 1600 sequences. Hierarchical clustering based on the weighted Unifrac distance metric (Lozupone et al. 2011) was computed by using Qiime (Caporaso et al. 2010) and visualizations were made in R (stats package v3.6.1). For phylogenetic analysis of the two most abundant OPUs, we selected 52 *pmoA* sequences from cultured and uncultured MOB published by Lüke and Frenzel (2011), Knief (2015) and in the NCBI GenBank (https://www.ncbi.nlm.nih.gov/). Sequences were aligned using MUSCLE implemented in MEGA 7 (Edgar 2004) and trimmed to retain only shared base pair positions. We built a best-scoring maximum likelihood phylogenetic tree (based on nucleotides) in Randomized Axelerated Maximum Likelihood (RAxML, version 8.2) using the General Time Reversible (GTR) Gamma model (Stamatakis 2014). Thereafter, OPU1 and 2 were aligned to the previously selected sequences and placed into the built phylogenetic tree using the Evolutionary Placement Algorithm implemented in RAxML. The resulting tree was visualized and annotated in Interactive Tree Of Life (Letunic and Bork 2016).

Results

Our data were collected during sampling surveys in the Arctic spring (May 2016, 2017, the month with the coldest bottom water temperatures; Berndt et al. (2014)), late spring (June 2016) and summer (July 2015). We mainly investigated a large seep area at the shallow shelf west of Prins Karls Forland and six additional regions, which are hydrographically connected to the Prins Karls Forland shelf area: Isfjorden (I–VII), Isfjorden Trough (VIII–X), and three stations towards the southern tip

of Svalbard: Outer Bellsundet (XI), Outer Hornsund (XII), and Sørkappøya (XIII). We collected discrete water samples for geochemical and microbiological analyses from eight defined water levels, whereas CTD measurements were made continuously throughout the water column. To simplify the following discussion about comparing processes at the ocean surface or close to the seafloor, we use the three main water layers, "Bottom Water Layer," "Surface Water Layer" and "Intermediate Layer" (as defined previously) in order to account for the differential water depth at the various stations.

Hydrographic setting

In May 2016, the entire water column was dominated by Transformed Atlantic Water with high salinity of 34.9–35.0 and temperatures between 1.6 and 2.3°C (Fig. 2A–D). In contrast, the water column in May 2017 was dominated by relatively warm (2–4.8°C) and saline (34.6–34.8) Atlantic Water. Water in the bathymetric depressions was slightly colder (2.3–2.8°C) and therefore classified as Transformed Atlantic Water (Fig. 2E–H). In June 2016, the bottom water was composed of Transformed Atlantic Water (lowest temperature 2.3°C) at the gas flare area (southern part of the western N-S transect) and within the bathymetric depressions, while we found warmer Atlantic Water (3–5°C) in the upper water column. Both water masses were characterized by salinities of 34.6–34.9 (Fig. 2I–K). A strong stratification was observed in July 2015 (Fig. 2L–O). At the bottom of the water column, specifically in bathymetric depressions, water was saline and relatively warm Atlantic Water (34.9, ~3.5°C) with fractions of Transformed Atlantic Water admixture. At the main gas flare

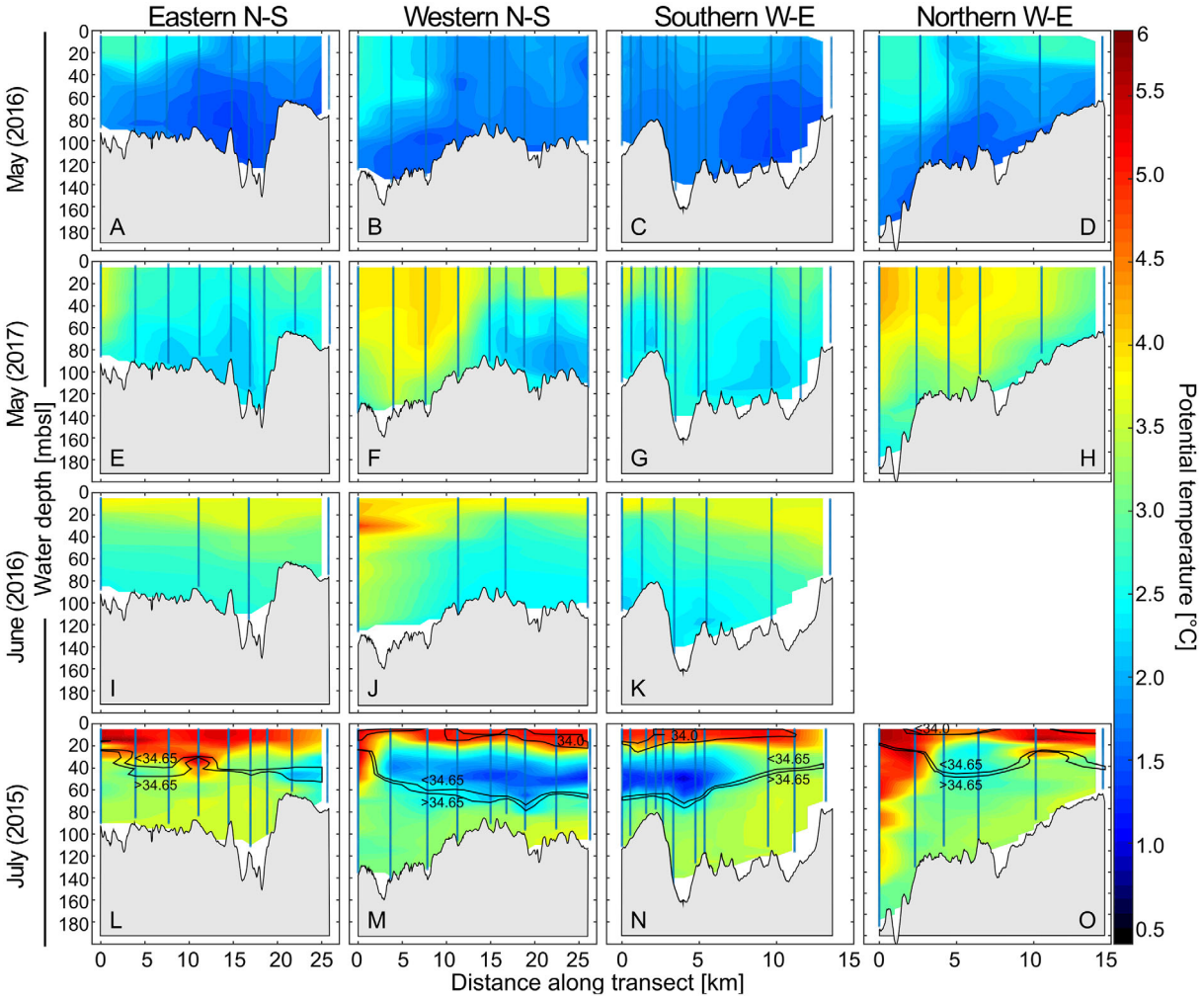

Fig 2. Profiles of potential temperature in the water column along transects at the shallow shelf west of Prins Karls Forland (**A–O**) from four sampling surveys in May, June, and July within three successive years (2015–2017). For each sampling survey, water depth on the *y*-axis is given in meters below sea level (mbsl). Vertical lines represent stations for continuous CTD measurements. The color code shows measured and linearly interpolated temperature values (°C). Selected salinity horizons (values in psu) are indicated by black lines in **L–O**. In May and June (**A–K**), no salinity horizons were observed due to a well-mixed water column with constant high salinity levels (34.6–35.0). Each plot contains the bathymetrical baseline (black line above gray area) characteristic for each transect. In June 2016, only three transects were conducted.

area, cold Intermediate Water (34–34.3, 1.3–2°C) lay above warmer Atlantic Water. Surface Water with temperatures of 4.5–5.5°C and low salinity (28.5–34.0) dominated the surface water down to ~20 m (Fig. 2L–M). The detailed hydrographic setting in May 2016 and July 2015 at the shelf west of Prins Karls Forland has been described by Silyakova et al. (2020).

At Isfjorden and Isfjorden Trough in May 2016, surface water temperatures were colder compared to the Prins Karls Forland shelf, i.e., between −0.2 and 1.2°C and with average salinities around 34.6, indicating Local Water and Intermediate Water formed due to local cooling and freshening over winter. Below the surface water layer, water salinity and temperature increased (> 34.86, 2.2–2.7°C) indicating that the Atlantic Water transformed into Transformed Atlantic Water in the fjord (Fig. S1A). The water column at the central stations of the Isfjorden Trough crossing transect (Stas. IV and V), was characterized by relatively warm Atlantic Water (35, 3.3°C) at the surface, which decreased in salinity and temperature to 34.8 and 1.6°C at 300 m water depth turning into Transformed Atlantic Water, indicating that at deeper depths, water masses were strongly influenced by mixing with West Spitsbergen Current waters. The lateral stations at the trough, i.e., those in proximity to the fjords sites, showed cold Surface Water (southern Sta. III: T = −0.2°C, S = 34.6; northern Stas. VI and VII: T = 0.7°C, S = 34.8), which turned into slightly warmer (2.2°C) and more saline water (34.9) at 35 m water depth, indicating that Surface Water lost more heat to the atmosphere than deeper waters, and that water was still mixing with the West Spitsbergen Current waters; Transformed Atlantic Water was dominating the deep-water column down to 365 m water depth (> 34.86, 1.6–2.7°C). Further inside Isfjorden (Stas. I and II), close to Longyearbyen, the entire water column was comprised of Local Water with salinity of 34.8 and temperatures of 0.8–1.2°C (Fig. S1A).

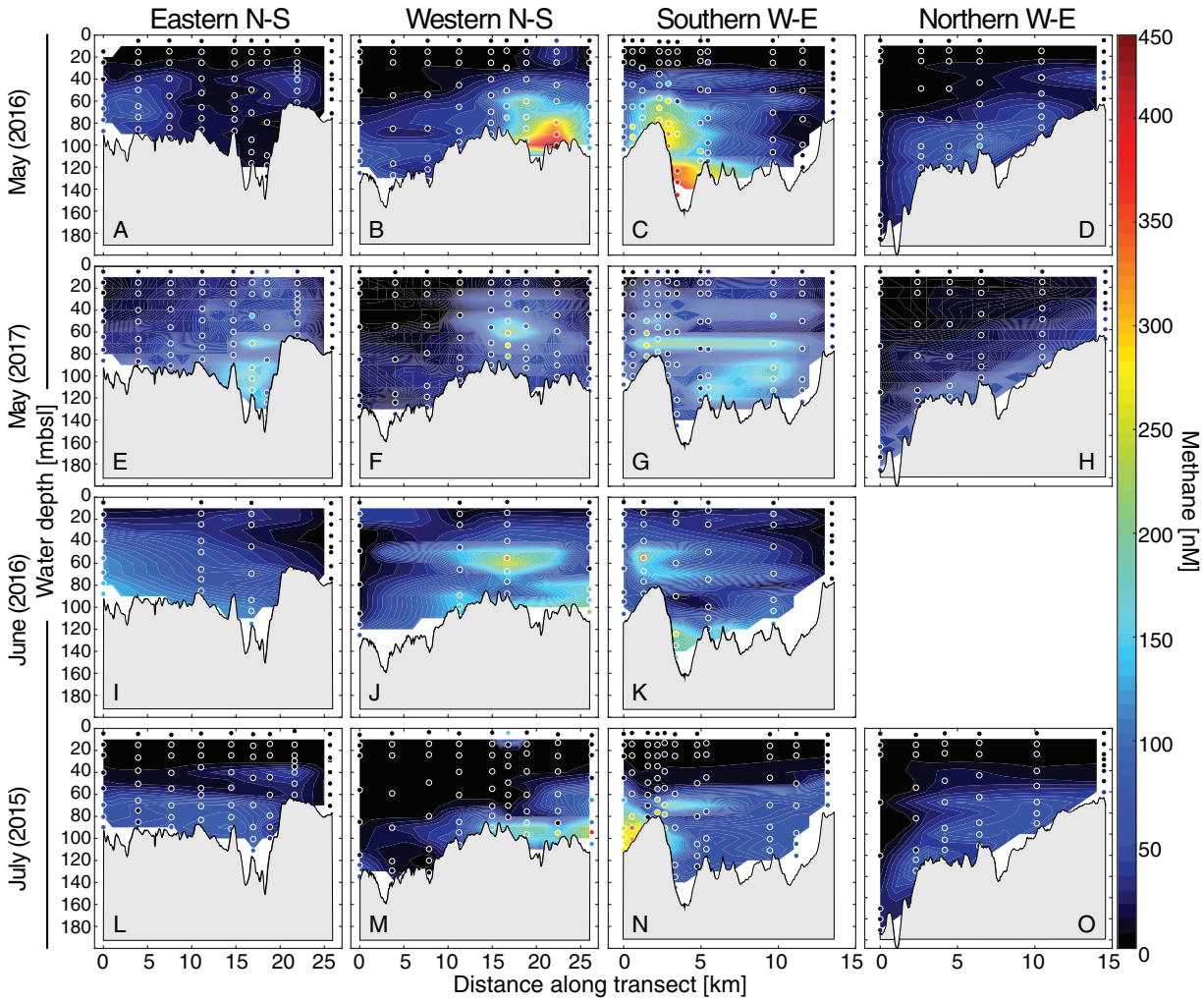

Fig 3. Profiles of dissolved CH_4 in the water column along transects at the shallow shelf west of Prins Karls Forland (**A–O**) from four sampling surveys in May, June, and July within three successive years (2015–2017). For each sampling survey, water depth on the *y*-axis is given in meters below sea level (mbsl). White circles represent single water samples. The color code shows measured and linearly interpolated CH_4 concentrations (nM). Each plot contains the bathymetrical baseline (black line above gray area) characteristic for each transect. In June 2016, only three transects were conducted.

In June 2016, Isfjorden surface waters down to 40 m were considerably fresher and warmer (34.2, 4.7°C) than in May 2016, most likely due to freshening through melting of glaciers, snow and sea ice and heating from the atmosphere (Fig. S1B).

Compared to Isfjorden in June 2016, a similar structuring of the water column was observed outside Bellsundet. In late June, surface temperatures were ~4°C, heated up by the atmosphere and surface salinities of 34.3–34.65 indicate the influence of Arctic Water, carried by the East Spitsbergen Current. Similarly, at Outer Hornsund, southwards from Bellsundet, surface salinity was not higher than 34.6, indicating the presence of Arctic Water transported by the East Spitsbergen Current (Fig. S1B).

Water column methane content

The entire water column was CH_4 oversaturated with respect to the atmospheric equilibrium concentration, which is ~ 3 nM at the ambient salinity and temperature conditions (Wiesenburg and Guinasso (1979) (Table S2). In the area west of Prins Karls Forland, we observed CH_4 plumes with concentrations of up to 437 nM. High concentrations were mainly encountered in bottom waters within the flare cluster, most dominantly in the southwest of the sampling grid, but the extent of the plumes differed greatly between the surveys (Figs. 3, S2). For example, we found elevated CH_4 concentrations extending widely from west to east in May 2017 (Fig. 3E–H) and June 2016 (Fig. 3I–K). In contrast, the eastward extension was less pronounced in May 2016 (Fig. 3A–D) and a clearly defined CH_4 plume was located at the intersection of the southern W-E and the western N-S transect (Fig. 3B,C). Nevertheless, the mean content of dissolved CH_4 in the water column was similar when comparing the different surveys (3483, 3547, and 3745 μmol m^{-2} in May 2016, May 2017, and July 2015, respectively) (Table 2, Fig. S2). In June 2016, the mean content of dissolved CH_4 reached 5644 μmol m^{-2} due to the reduced number of stations (12 out of 64 stations) that were sampled during this survey, and that many of the sampled stations were located above active flares (see sampling strategy), which in turn translated to higher mean values (see the calculated mean content of dissolved CH_4 for the reduced number of stations for all surveys in Table S2). Therefore, dissolved CH_4 values from June 2016 are not directly comparable to values from the other surveys.

In general, CH_4 concentrations were highest in bottom waters, translating to inventories that were also highest at the Bottom Water Layer (2127–2867 μmol m^{-2}) compared to the Intermediate (795–1008 μmol m^{-2}) and Surface Water Layer (83–412 μmol m^{-2}) (Table 2).

At Isfjorden (Stas. I and II) we observed elevated concentrations of 26 and 57 nM (May and June 2016, respectively) in the Bottom Water Layer, whereas at the Isfjorden Trough CH_4 was generally low, with average values of 9 nM in the Bottom and 3 nM in the Surface Water Layer (May 2016). At Outer Bellsundet, Outer Hornsund and Sørkappøya, CH_4 concentrations in the Bottom Water Layers were 18, 12, and 24 nM, respectively, and 11, 4, and 17 nM in surface waters (Table S2).

Methane oxidation activity

Highest MOx activity was generally found in bottom waters, although the magnitude of activity greatly varied

Table 2. Inventory of dissolved CH_4 and microbial methane oxidation activity calculated for the sampling area at the shallow shelf of Prins Karls Forland. Surface, Intermediate, and Bottom refers to the defined water layers (Table 1) of the water column. Total values are the sum of all three water layer values per sampling campaign. The order of sampling campaigns in this table follows the cycle of the seasons where May corresponds to Arctic spring and July to summer.

	Dissolved methane				Methane oxidation activity					
	Surface	Interm.	Bottom	Total	Surface	Interm.	Bottom	Total	CH_4 oxid. per day*	100% turnover**
	Mean content (μmol m^{-2})				Mean turnover (μmol m^{-2} d^{-1})				(%)	(d)
May (2016)	100	928	2456	3483	0.006	0.18	0.33	0.51	0.015	6777
May (2017)	412	1008	2127	3547	0.104	0.48	1.46	2.02	0.057	1754
July (2015)	83	795	2867	3745	0.089	1.73	25.72	27.54	0.735	136

	Dissolved methane				Methane oxidation activity			
	Surface	Interm.	Bottom	Total	Surface	Interm.	Bottom	Total
	Total content in the area ($\times 10^5$ mol)				Total turnover in the area (mol d^{-1})			
May (2016)	0.37	3.38	8.94	12.68	2	65	120	187
May (2017)	1.50	3.67	7.74	12.91	38	173	532	736
July (2015)	0.30	2.89	10.44	13.63	32	630	9362	10,024

*Percentage of CH_4 that is oxidized per day.
**Time in days that it would take to totally oxidize the available CH_4.

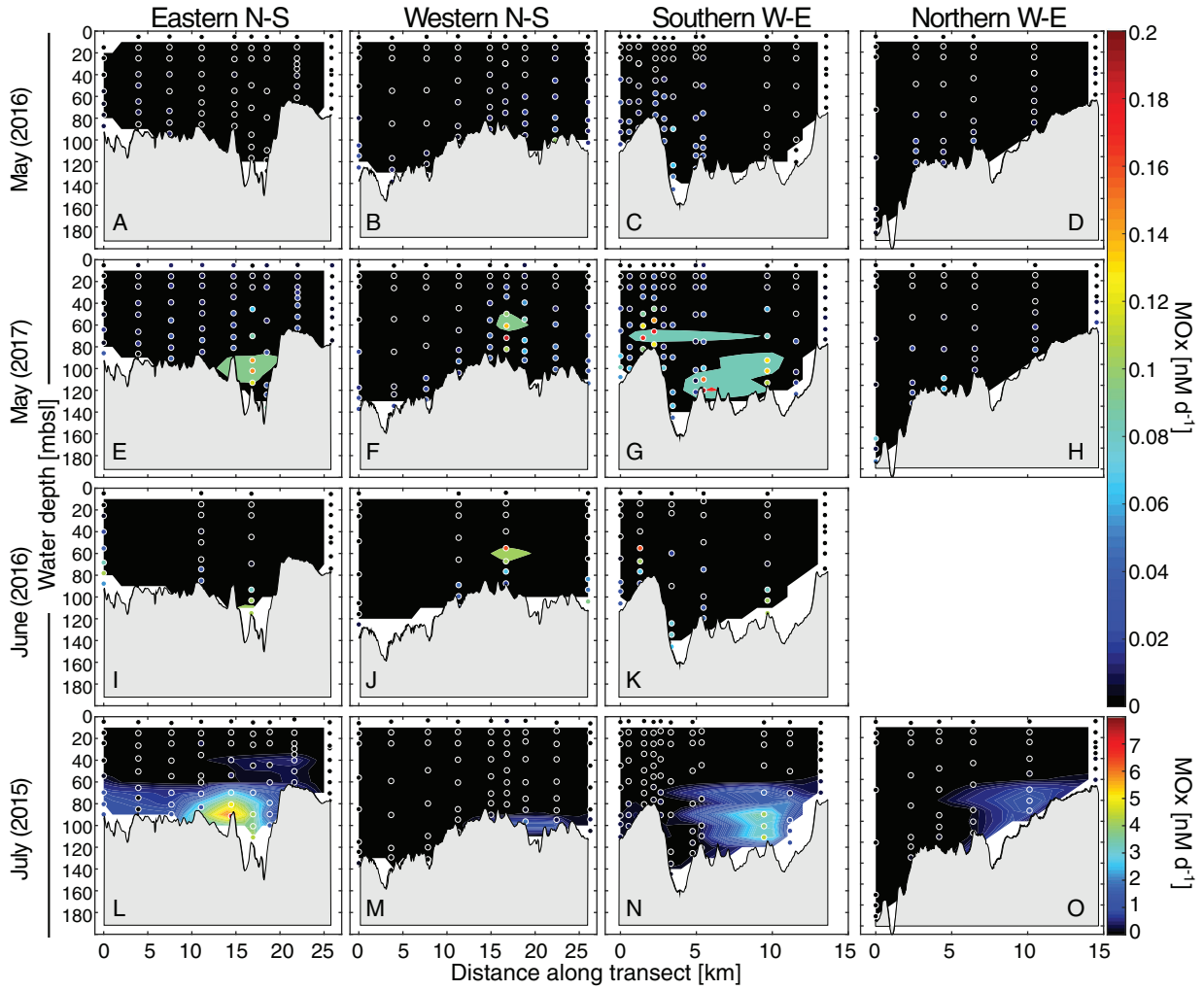

Fig 4. Profiles of microbial CH_4 oxidation (MOx) rates in the water column along transects at the shallow shelf west of Prins Karls Forland (**A–O**) from four sampling surveys in May, June, and July within three successive years (2015–2017). For each sampling survey, water depth on the *y*-axis is given in meters below sea level (mbsl). White circles represent single water samples. The color code shows measured and linearly interpolated MOx rates (nM d^{-1}). Each plot contains the bathymetrical baseline (black line above gray area) characteristic for each transect. In June 2016, only three transects were conducted. Note that we have used the same interpolation settings for all transects (with a resolution of 0.1 nM d^{-1}), but have chosen two color scales for the July vs. May and June expeditions.

between surveys (Figs. 4, S3). We found a MOx maximum value of 7.1 nM d^{-1} in the south-east part of the sampling area at the Prins Karls Forland shelf in July 2015 (Sta. 53; Fig. S4). In contrast, MOx maxima in May 2016, May 2017 and June 2016, were more than an order of magnitude lower with values of 0.09, 0.16, and 0.23 nM d^{-1}, respectively (Fig. S4). Similarly to maximum rates, depth integrated MOx activity in the Bottom Water Layer was also highest in July 2015 (25.72 nmol m^{-2} d^{-1}) and substantially lower in May 2016 (0.33 nmol m^{-2} d^{-1}), May 2017 (1.46 nmol m^{-2} d^{-1}) and June 2016 (1.67 nmol m^{-2} d^{-1}). In the Surface Water Layer, average MOx activity was generally below 0.1 nmol m^{-2} d^{-1} (Table 2, Fig. S3).

Among the stations along the transect inside Isfjorden, highest MOx activity was in the bottom waters at Sta. I (0.04 nM d^{-1} in May and 0.5 nM d^{-1} in June 2016 (Fig. S4); no samples were taken in Isfjorden in 2015). MOx rates at Outer Bellsundet, Outer Hornsund and Sørkappøya were < 0.04 nM d^{-1} (Table S2).

Methanotrophic community

The particulate methane monooxygenase gene (*pmoA*) was sequenced from selected bottom water samples with elevated MOx rates. The selected samples originated from the flare area (Sta. 9 May 2016 and 10 July 2015), the bathymetric depression zone (Stas. 54 May, June 2016, July 2015 and 58 May 2016, July 2015), Sta. 49 located at the north-east corner of the sampling grid (May 2016 and July 2015), Sta. I at Isfjorden (May and June 2016), and from Outer Bellsundet (Sta. XI June 2016) (Fig. 1, Table S1). The number of generated *pmoA* sequences ranged

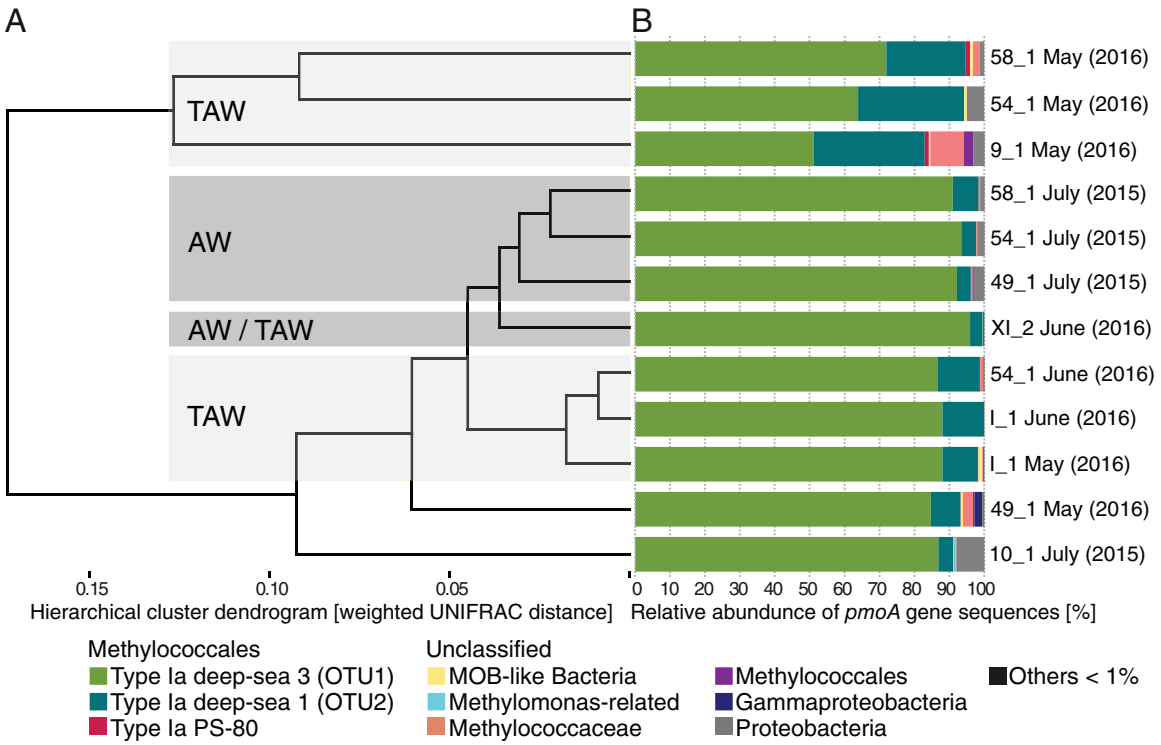

Fig 5. Hierarchical clustering of OPUs derived from *pmoA* gene sequences (**A**) and relative abundance (**B**) of the methanotrophic community from selected stations from the shallow shelf of Prins Karls Forland, Isfjorden (I) and Outer Belsundet (XI) investigated over three sampling surveys in May 2016, June 2016, and July 2015. Sample IDs derive from the station number (see sampling grid in Fig.1B) and water levels (1: 5 m above seafloor, 2: 15 m above seafloor). Gray squares show predominant water masses found at the bottom water level at the stations (AW: Atlantic Water, TAW: Transformed Atlantic Water).

from 20,132 to 44,469 per sample. After processing, quality reads clustered into 70 OPUs with absolute abundance of maximum 34,299 and minimum 424 reads across samples. The most abundant OPUs were related to the gammaproteobacterial deep-sea 3 and deep-sea 1 clades, both of which are subgroups of gammaproteobacterial Methylococcaceae Type Ia MOB according to Lüke and Frenzel (2011) (Figs. 5, S6). In bottom water samples from May 2016, the relative abundance of Type Ia deep-sea 1 MOB was higher compared to the other months. In addition, OPUs belonging to unclassified Proteobacteria or Methylococcaceae-related genera only showed low sequence abundance.

Bacterial diversity

Our 16S rRNA gene analyses of water column bacterial community compositions revealed a great phylogenetic diversity and spatial variability. After sequence processing of > 1.2 million raw sequences from 57 samples, 11,705 OTUs were generated.

The majority of the 16S rRNA gene sequences clustered into OTUs which are taxonomically affiliated with Alphaproteobacteria (34%), Gammaproteobacteria (30%), Bacteroidetes (25%), and Verrucomicrobia (4%) (Fig. 6B). Among the Alphaproteobacteria, the most abundant families were SAR11 clade I, SAR11 clade II and Rhodobacteraceae (*Planktomarina* and *Sulfitobacter*). Relatives of Gammaproteobacteria were mainly affiliated with Nitrincolaceae, Thioglobaceae, SAR86 clade, Porticoccaceae, and Methylophagaceae. The majority of the Bacteroidetes sequences were classified as Flavobacteriaceae with the dominant genera *Polaribacter* 1, *Polaribacter*, NS5 marine group, and *Aurantivirga*. Other abundant Bacteroidetes were NS9 marine group, Cryomorphaceae and Bacteroidaceae. Among the Verrucomicrobia, Rubritaleaceae was the most abundant family. Sequences affiliated with *Luteolibacter* and *Roseibacillus* were present in low amounts in almost all samples, but slightly more abundant in bottom waters sampled in July 2015.

Only few 16S rRNA gene sequences were associated with known methanotrophic or methylotrophic bacteria OTUs (related to either Alpha- or Gammaproteobacteria; Fig. 6D). Known MOB found in the data set were related to clade Milano-WF1B-03 (6 OTUs; Heijs et al. (2005)), found in samples from bottom waters at Stas. 54 and 58 in July 2015 and at station IF in May and June, and to the *Methyloprofundus* clade (4 OTUs) found at Stas. 9 and 19 sampled in May 2016. Furthermore, OTUs affiliated to *Methylobacterium*, *Methyloceanibacter*, and unclassified Methylomonaceae (one OTU each) were identified.

Methylotrophs were represented by members related to uncultured Methylophagaceae (110 OTUs in total) present in samples from the shelf west off Prins Karls Forland taken in June 2016 and July 2015; one OTU was identified as *Methylophaga* and found at Sta. I, Isfjorden. *Methylotenera* (two OTUs) was encountered in the whole water column in July 2015 and other genera of the family Methylophilaceae (OM43 clade, 72 OTUs) were present at all seasons. Known MOB accounted for 0.05% of all sequences, and known methylotrophs accounted for 1.08% of all sequences (Fig. 6D).

Community beta diversity analysis revealed the time of sampling (sampling campaign) as one dominant factor shaping the bacterial community composition (envfit, $p \leq 0.05$). The dissimilarity of the bacterial community was particular apparent in samples retrieved in May 2016 (spring) compared to samples from June 2016 and July 2015 (late spring/summer; Fig. 7A). In addition to the sampling campaign, water depth was a second variable that significantly correlated with community dissimilarity ($p \leq 0.05$). To reduce the masking of seasonal effects on the beta diversity analysis, we subsequently focused on samples retrieved from single sampling campaigns. Here, water temperature and depth, both independent environmental variables, influenced the communities ($p \leq 0.05$). Since these factors/variables (together with salinity) also define the classification of water masses (see section Hydrographic setting), water masses are indicated in Fig. 7B–D. In June 2016 and July 2015, communities revealed similarities according to water masses (Fig. 7C,D). Analogously, medium or high active MOB communities were more similar to one another. At Isfjorden and Outer Bellsundet, where water mass properties were highly affected by local features, communities were distinctively different to most of the other communities found at the shelf west off Prins Karls Forland, especially in June 2016 (Fig. 7C).

Supplementing NMDS-based analysis, we conducted canonical correspondence analysis (CCA). Similar to NMDS, CCA also indicated that water temperature, depth, and salinity significantly influenced the community composition (Table 3). For the bacterial communities in May and June 2016, these environmental variables adequately described the variation of the community composition, as supported by a significant level for the CCA Model (ANOVA; $p \leq 0.009$ and $p \leq 0.002$, respectively). In contrast, the composition of samples retrieved in July 2015 showed a much higher variation than could adequately be explained by the investigated environmental variables included in the model ($p \leq 0.129$), suggesting that additional unidentified factors played a major role. When taking community-dependent variables into account, such as amount of extracted DNA and CH_4 oxidation, both correlated with the identified communities (Table 3).

To identify a possible correlation of bacterial phyla with methane oxidation rates, we conducted a Spearman's rank correlation analysis on family level. Following clades depicted the greatest positive correlations: unclassified members of the OCS116 clade, Nitrosomonadaceae, Cellvibrionaceae, clade OM182, clade ZD0405, Thiothrichaceae, Rubritaleaceae, and Verrucomicrobiaceae (Fig. S7). Many of these families also depicted a positive correlation with CH_4 concentration and water level. Methane concentration, water depth and methane oxidation rates were also strongly correlated with another.

Repeated sampling

Hydrographical parameters (salinity, temperature, pressure), concentration of dissolved CH_4 and MOx activity were repeatedly measured at Stas. 9, 16, 31, 44, 54, and 64 over a 2-day time period (Table S1). Water mass properties only showed marginal differences (Fig. S8A,D). Stations located above or close to the flare area (Stas. 9, 19, 31, and 44) showed stronger variations in CH_4 concentrations in samples from greater water depths. MOx activity rates from all six stations (Fig. S8C,F) in addition to the 16S rRNA gene sequencing results from Sta. 9, showed high similarities when comparing the two time points (Fig. 6B).

Discussion

The shallow shelf west off Prins Karls Forland is characterized by numerous gas flares at the ridge of the Forlandet moraine complex as well as the many bathymetric depressions extending eastwards from the moraine. The water column at the shallow shelf is a hydrographically complex and dynamic system with seasonal variations in water mass properties. Individual gas flares transport differential amounts of CH_4 into the water column, and total CH_4 flux on the shelf also varies over time (Silyakova et al. 2020). However, a seasonal connection with high CH_4 fluxes during the warm season and ~ 80% lower fluxes during cold bottom water conditions, as found at the shelf break below 360 m water depth (Ferré et al. 2020), is not evident on the shallow shelf, where active flare clusters occur at 90 m. Such a depth is far above the uppermost limit of the shifting gas hydrate stability zone, which was found to be in between 380 and 400 m water depth (Berndt et al. 2014). We repeatedly investigated the shallow shelf over a time period of 3 years covering the Arctic spring (May 2016, 2017), late spring (June 2016) and summer (July 2015) and their specific hydrographic conditions. Our study reveals the activity, distribution and structure of methane-oxidizing communities in the water column on the shallow shelf west of Svalbard.

Spatiotemporal variations of methane content in the entire water body

Similar to previous studies on CH_4 dynamics in coastal waters of Svalbard (e.g., Damm et al. 2005; Graves et al. 2015; Mau et al. 2017), we generally observed highest CH_4 concentrations in bottom waters. In our sampling grid west of Prins Karls Forland (Fig. 1B), CH_4 concentrations frequently exceeded 100 nM in particular at gas flares locations (Fig. 3). Methane concentrations in surface waters were supersaturated compared to atmospheric concentrations across all surveys

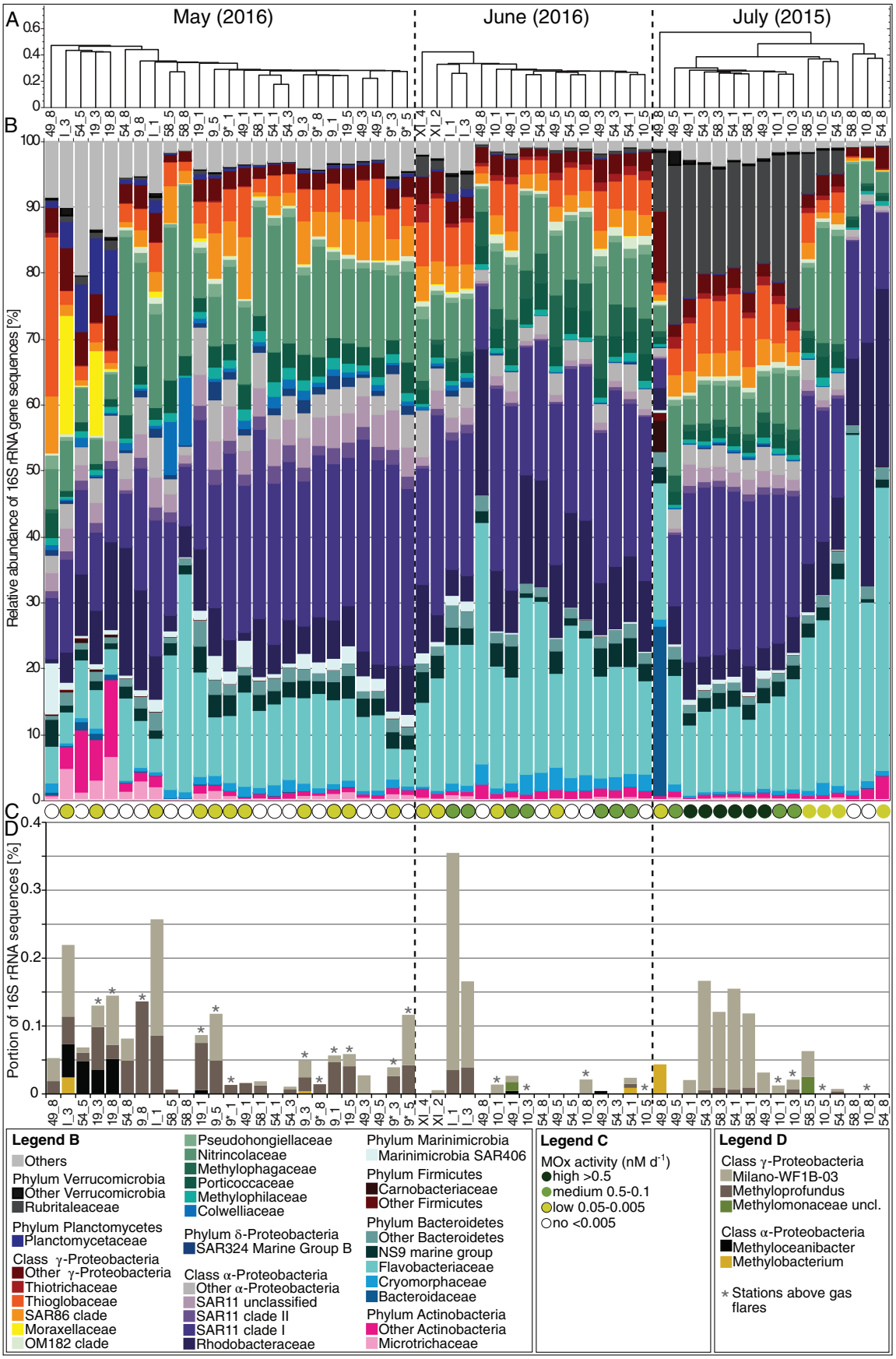

Fig 6. Legend on next page.

(1–5 fold on average). However, substantial impacts on atmospheric CH_4 concentrations in the region of the western Svalbard continental margin could not be confirmed (Myhre et al. 2016).

Furthermore, the integrated CH_4 inventory of the three water layers of the sampling grid during the surveys in spring (May 2016 and 2017), late spring (June 2016) and summer (July 2015), shows up to three times higher CH_4 values at the Bottom Water Layer compared to the Intermediate and Surface Water Layers, as a result of the CH_4 seepage from the seafloor (Table 2, Fig. S2). Moreover, the total content of dissolved CH_4 in the area (423 km^2) is consistent with values of ~ 13×10^5 mol $area^{-1}$ in spring (May 2016/17) and summer (July 2015). The seemingly high total CH_4 content in late spring (June 2016) is caused by an under-sampling of the survey area (see section Water column methane content and Study area and Sampling strategy).

Our values from May 2016/17 and July 2015, together with previously published flux data (Silyakova et al. 2020), indicate comparably steady CH_4 inputs in our study area during the investigated seasons. In contrast, seep activity in deeper water levels at the shelf break are strongly reduced during times with low bottom water temperatures (Ferré et al. 2020), because the uprising CH_4 "freezes out" as gas hydrate in surface sediments, building up a seasonal gas hydrate capacitor that is reduced in summer.

Moreover, our repeated sampling over the short time period of 2 days in May 2016 showed negligible variations in CH_4 concentration and water mass properties (Fig. S8A,D), and neither the bacterial MOx activity (Fig. S8C,F) nor the community composition (Fig. 6B) revealed any remarkable differences between the two time points. These findings indicate that hydrographic and biogeochemical variations during one sampling of the entire grid were most probably low (Steinle et al. 2015).

Spatiotemporal variations of methane oxidation activity

Methane oxidation in the ocean is the final sink for dissolved CH_4 before its release into the atmosphere (e.g., Reeburgh 2007; Steinle et al. 2015). Previous studies report that elevated MOx activity in marine environments is related to high CH_4 concentrations (Valentine et al. 2001; Mau et al. 2013; Crespo-Medina et al. 2014; Steinle et al. 2015). In our study, we also found elevated MOx rates in methane-rich bottom waters. But in the CH_4 plumes, MOx was not substantially elevated (Figs. S2, S3). This has been found elsewhere, too (Crespo-Medina et al. 2014; Steinle et al. 2015, 2017), and a literature review only revealed a correlation of MOx and CH_4 contents on logarithmic scales (James et al. 2016). The rather loose dependency of MOx and CH_4 concentrations indicates that microbial community abundance, and possibly other factors such as the availability of micronutrients, seems at least equally important in determining the efficacy of the microbial CH_4 filter in the water column (Steinle et al. 2015).

Our study area is characterized by steady CH_4 contents between seasons, but similarly to the spatial variation of MOx within one sampling campaign, we found large seasonal differences in MOx activity. In the Arctic spring (May) and late spring (June), MOx rates were generally low (weighted mean: < 2.02 μmol m^{-2} d^{-1}; total MOx: < 736 mol d^{-1}; Table 2). In contrast, in summer (July), MOx in the entire area was about one order of magnitude higher (weighted mean: 27.54 μmol m^{-2} d^{-1}; total MOx: 10,024 mol d^{-1}). It is also noteworthy that the maximum MOx value measured in summer (July; 7.2 nM d^{-1}) was much higher compared to previous measurements conducted in the area around Svalbard. Steinle et al. (2015) measured MOx rates of up to 3.2 nM d^{-1} at the continental slope west of our study area in Arctic summer (August). Mau et al. (2017) published rates of up to 2.2 nM d^{-1} in a CH_4 plume located more southerly between Hornsundbanken and Isfjordbanken west of Spitsbergen from the same season (August/September).

We discovered that the capacity of MOx shows a high spatiotemporal variation. The high MOx rate in summer translates to a turnover time of the CH_4 inventory of the entire sampling grid (13.63×10^5 mol) of about 136 d. In contrast, the turnover time was substantially longer in spring (1754–6777 d). While MOx plays a substantial role in retaining CH_4 in the Arctic summer, it seems of rather lower importance in winter. Similar seasonal differences were also found at the shelf break west of our study area (Steinle et al. 2015; Ferré et al. 2020). In general, the turnover times at the Prins Karls Forland shelf are within the intermediately high to low range when compared to previously reported turnover times of weeks to a few years from methane-rich, Arctic waters (Mau et al. 2013; Steinle et al. 2015; James et al. 2016). Turnover times of several decades are rare and typically restricted to oceanic deep waters with very low CH_4 contents (< 10 nM) (Rehder et al. 1999; Heeschen et al. 2003; James et al. 2016).

Fig. 6. Differential bacterial community structure based on 16S rRNA genes investigated over three sampling surveys of the shelf west of Prins Karls Forland, Isfjorden and Outer Belsundet. (**A**) Hierarchical clustering of bacterial communities of each sampling survey is based on subsampled Bray–Curtis dissimilarity matrix (OTU) and the complete linkage method. Stability of clusters was tested by bootstrapping 1000 times. (**B**) Relative abundance of bacteria based on 16S rRNA gene sequences are sorted according the hierarchical clustering within each sampling survey. Only taxa with abundances of >1% of total sequences are shown. (**C**) Simplified ranking of measured methane oxidation (MOx) activities per sample. (**D**) Proportion of 16S rRNA sequences, which were assigned to methanotrophic bacteria. Sample IDs are derived from the station number (see sampling grid in Fig. 1B) and water levels (1: 5 m above seafloor, 3: 25 m above seafloor, 5: Intermediate water level, 8: 5 m below sea surface, I: Isfjorden, XI: Outer Belsundet). Sta. 9 was repeatedly sampled during the sampling campaign; repeated samples are therefore marked with asterisks (9*_1 to 8).

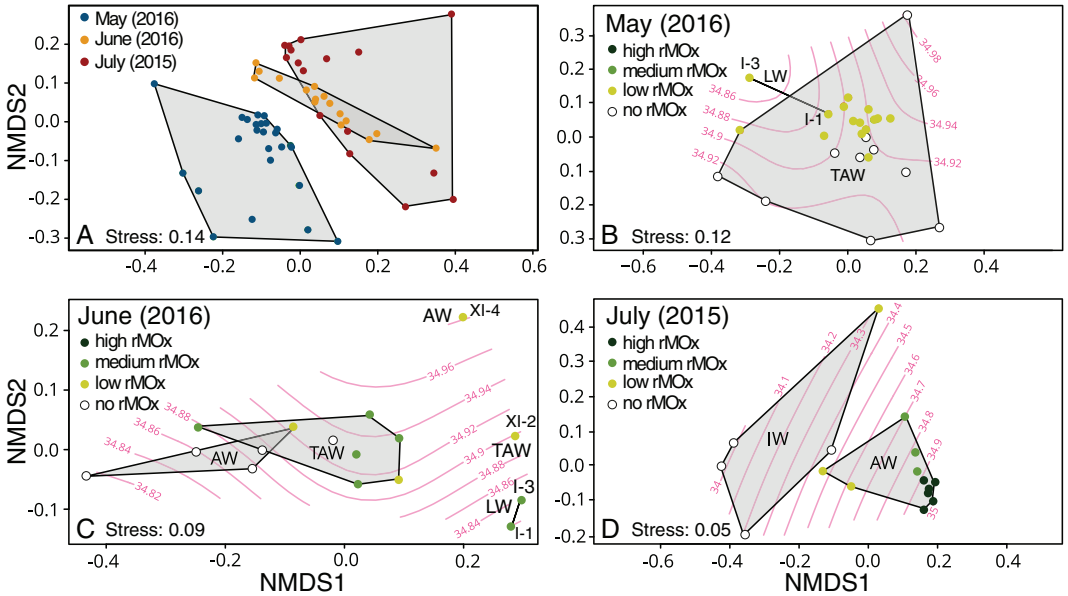

Fig 7. Seasonal correlation of microbial communities from all samples retrieved from all sampling surveys (**A**) and between microbial communities and salinity (red lines and values) according to single sampling campaigns (**B–D**). Non-metric multidimensional scaling (NMDS) derive from the Bray–Curtis dissimilarity index. AW: Atlantic Water; TAW: Transformed Atlantic Water; LW: Local Water; IW: Intermediate Water; I: Isfjorden (water levels 1 and 3); XI: Outer Bellsundet (water levels 2 and 4). Methane oxidation rates (rMOx) are defined as high: >0.5, medium: 0.5–0.1, low: 0.05–0.005, no: <0.005 nM d^{-1}.

Table 3. Canonical correspondence analysis (CCA) significance values of independent and dependent variables. Values marked with * indicate values of significance. Temp: temperature; Fluor: fluorescence; CH_4: dissolved methane concentrations; DNA: 16S rRNA gene sequencing analysis; MOx: methane oxidation rates. The order of sampling campaigns in this table follows the cycle of the Arctic seasons where May corresponds to spring, June to late spring, and July to summer.

		Independent variables					Dependent variables	
	ANOVA, CCA model	Temp.	Depth	Salinity	Fluor.	CH_4	DNA	MOx
May (2016)	0.009*	0.005*	0.050	0.315	0.155	0.275	0.560	0.030*
June (2016)	0.002*	0.005*	0.005*	0.150	0.015*	0.580	0.025*	0.005*
July (2015)	0.129	0.025*	0.005*	0.005*	0.465	0.165	0.005*	0.035*

Hydrographical dynamics on the shelf

The spatiotemporal variations of CH_4 content and MOx activity indicate two contrasting mixing regimes at the shelf, both of which have profound effects on MOx activity as well as the bacterial community composition.

The first scenario is characterized by a water column dominated by Atlantic Water as it was typically the case in summer (July; Fig. 2L–O). Atlantic Water episodically floods the shallow shelf in the form of numerous eddies caused by the West Spitsbergen Current that meanders eastwards onto the shelf (Nilsen et al. 2008; Steinle et al. 2015). The dense Atlantic Water replaces the shelf water, less saline (though colder) Arctic Water brought by the East Spitsbergen Current, and fills up the bathymetric depressions (Silyakova et al. 2020). This phenomenon was particularly apparent at the eastern end of the southern W-E transect, where the depressions are 40 m deeper than the surrounding seafloor. There, we found hot spots of MOx activity with 2–3 times higher rates than those reported previously from the continental shelf around Svalbard (Mau et al. 2013; Gentz et al. 2014; Steinle et al. 2015, 2017) although CH_4 concentrations were only moderately high in the depressions compared to gas flare locations in the western part of the sampling grid (Figs. S2, S3). Prior to flooding the shelf, Atlantic Water has an offshore history where CH_4 concentrations are low (Steinle et al. 2015). When swept over the CH_4 seeps at the shelf break (i.e., west of the study area), Atlantic Water becomes charged with CH_4, but MOx rates in the water column are initially low because of the initially low MOB content in this water mass (Steinle et al. 2015). When reaching the depressions, methane-enriched Atlantic Water becomes trapped as these depressions provide a sheltered environment with long residence times. This supports MOB

community growth and leads to an elevated MOx capacity (James et al. 2016). Due to the hydrographic complexity of the area, the frequency at which these depressions are filled with dense Atlantic Water and how frequently they are flushed with water of different origins, remains unknown.

The second scenario is characterized by frequent water mass shifts as a result of intense mixing in the study area. Mixing is furthermore responsible for the dispersion of dissolved CH_4. Meandering of the West Spitsbergen Current, flooding and flushing of the shallow shelf occur more often in winter and spring (von Appen et al. 2016; Silyakova et al. 2020). Moreover, the upwelling of Atlantic Water onto the shelf and into fjords in winter enhances the mixing of Transformed Atlantic Water and Local Water that reside there (Cottier et al. 2007). Arctic Water, often together with sea ice floes, both transported with the East Spitsbergen Current from the Northern Barents Sea (Nilsen et al. 2016) additionally contribute to the residing water mass replacement. The frequent mixing does not provide stable conditions for microbial community development. In other words, the short residence times and the frequent exchange of water masses in the bathymetric depressions with water masses containing only low amounts of MOB leads to an overall low abundance of water column MOB and thus MOx activity, which is less effective in retaining CH_4. In contrast, the CH_4 charged water masses are transported away from the CH_4 point sources and disperse in the lee of the seep (Graves et al. 2015). Consequently, we only observed low MOx activity in spring (Fig. 4A–H).

Composition of the methane-oxidizing bacterial community

We evaluated the methanotrophic and other methylotrophic communities in bottom water level from stations located at the shelf west off Prins Karls Forland (Stas. 9, 10, 49, 54, and 58), Isfjorden (I) and Outer Bellsundet (XI), which were collected in the Arctic spring and late spring (May and June), and summer (July). These samples were selected for *pmoA* gene amplicon sequencing because of their elevated MOx rates, which suggested the presence of active MOB.

The prevalent members of the MOB community in all samples, and irrespective of the water mass, were dominated by Type Ia deep-sea 3 MOB (OPU1) with variable but minor shares of Type Ia deep-sea 1 MOB (OPU2; Fig. 5B). OPU1 shares 98% sequence similarity with an uncultured MOB from the water column above the Oregon seep system at Hydrate Ridge (sequence FJ858282, GenBank; Hansman et al. (2017); Fig. S6). OPU2 shares 92% sequence similarity with *Methyloprofundus sedimenti* (sequence KF484908; Tavormina et al. (2015); relating to the family level, Yarza et al. (2014)), which is a known obligate MOB of the family Methylomonaceae, isolated from marine surface sediment from Monterey Canyon off the coast of California (USA) (Fig. S6). Both, the deep-sea 1 and 3 subgroups, mainly constitute mesophilic uncultured MOB from marine and freshwater environments (Lüke and Frenzel 2011; Knief 2015; Hansman et al. 2017). Our data show that a higher percentage of Type Ia deep-sea 3 MOB (OPU1) was found in Atlantic Water and Atlantic Water/Transformed Atlantic Water, i.e., the water mass prevailing in the bathymetric depressions where we also found high MOx activities. This suggests that Type Ia deep-sea 3 MOB is the main driver for active MOx in our study area.

The majority of the identified OTUs from the 16S rRNA gene sequences are related to heterotrophic bacteria that are often found to be the predominant representatives of bacterioplankton communities worldwide, seemingly having a major ecological role in marine food webs (Giovannoni and Stingl 2005). Where instead the relative abundance of MOB in the total bacterial community is low (0.05% of the total 16S rRNA gene sequences) and therefore comparisons among MOB should be considered with care. The presence of OTUs related to *Methyloprofundus* sp. and Milano-WF1B-03, the two most abundant MOB in the 16S rRNA data set, coincide with the locations of MOx hot spots—in the depression in summer (July) and above CH_4 flares in spring (May) (Fig. 6C,D). OTUs related to the known methylotrophs (Methylophagaceae: *Methylophaga* and Methylophilaceae: *Methylotenera* and OM43 clade), which are present in all of our samples, were frequently found in marine and freshwater ecosystems where they profit from C1-compounds, such as methanol and methylamine, released as a product of methane monooxygenase activity of MOB (Neufeld et al. 2007, 2008; Moussard et al. 2009). However, it also has been suggested that Methylophilaceae species might be able to incorporate CH_4 directly (Redmond et al. 2010).

We also identified high abundances of sequences affiliated with Verrucomicrobia (Fig. 6B). Members of this phylum have been found globally in a variety of aerobic and anaerobic marine environments (Freitas et al. 2012), but only a few species were isolated and characterized so far, and relatively little knowledge exists on the metabolic capabilities of Verrucomicrobia. We found members of the family Rubritaleaceae genus *Luteolibacter*, which are highly abundant in samples associated with high MOx activity (July 2015, primarily in the bottom water level; Fig. 6B). *Luteolibacter* comprises six known species that are described as chemoheterotrophs utilizing a variety of carbon sources (Zhang et al. 2017). None of them has been tested for MOx activity and to the best of our knowledge, no genome data from this genus are available. Yet, some other members of the Verrucomicrobia ("Ca. *Methylacidimicrobium*," "Ca. *Methylacidiphilum kamchatkense*" strain Kam1, V4 and SolV) were found to mediate MOx (Dunfield et al. 2007; Pol et al. 2007; Kruse et al. 2019). Methanotrophic Verrucomicrobia have multiple operons encoding the particulate methane monooxygenase with identical *pmoCAB* operon structure when compared to proteobacterial MOB (Op den Camp et al. 2009). However, despite the similar operon structure, no standard *pmoA* primer set can amplify verrucomicrobial *pmoA* genes, which seems to be only detectable by shot-gun genome

sequencing (Dunfield et al. 2007; Pol et al. 2007). As a result, the abundance, distribution and diversity of Verrucomicrobia MOB has been overlooked in most ecological studies (Bergmann et al. 2011). We did not detect any Verrucomicrobia-related species with our *pmoA* sequencing approach and although the obvious co-occurrence of *Luteolibacter sp.* (class Verrucomicrobia) with high MOx rates shown here is remarkable, we can only speculate if the *Luteolibacter* at the Prins Karls Forland shelf are involved in MOx (directly or indirectly) or if their abundance maximum is related to factors that are independent of CH_4-dynamics.

Origin of methane-oxidizing bacteria

The meandering of the West Spitsbergen Current causes occasional flooding events of the shallow shelf at Prins Karls Forland with Atlantic Water (Steinle et al. 2015; Silyakova et al. 2020). Because of the general south–north direction of the West Spitsbergen Current, it thus seems likely that the residual Atlantic Water that we found in the bathymetric depressions in summer had, before being trapped in the bathymetric depressions, passed our southern stations, i.e., Outer Bellsundet, Outer Hornsund, and Sørkappøya. At these stations, we found elevated CH_4 concentrations around seeps, which were discovered along the Svalbard margin (Mau et al. 2017). Furthermore, we found high similarities between the MOB communities found at the shallow shelf offshore Prins Karls Forland and at the southern stations (Fig. 5A). For example, the MOB communities at Stas. 49, 54 and 58 (all offshore Prins Karls Forland) in summer (July 2015) comprise more than 90% of Type Ia deep-sea 3 MOB, just like the MOB community at Outer Bellsundet in late spring (June 2016; Fig. 5B). The bottom water layers of all southern stations were characterized by the influence of warm and saline Atlantic Water (similar to the bathymetric depressions offshore Prins Karls Forland in the summer).

Wilkins et al. (2013) suggested that the advection of microorganisms originating from upstream-locations, which then colonize sites downstream, shape the microbial community at the downstream locations. It also appears that increasing opportunities for colonization (and subsequent growth) are more relevant than the numbers of transported organisms. Translated to our study, this converts into the following: the microbes from Outer Bellsundet (upstream site) colonize the shelf west of Prins Karls Forland (downstream site). The specific hydrographic setting at the downstream site, i.e., sheltered conditions comprising CH_4 and nutrient-rich water that is trapped in the depressions due to flooding events and strong stratification of the water column in summer allows MOB communities to develop. These factors are then also more important than the sheer number of MOB cells being transported from the southern stations to the Prins Karls Forland shelf. Moreover, the inoculation theory leads to the assumption that the blooming MOB community from the Prins Karls Forland shelf could be in turn an inoculum for other "MOx systems" further north, and that seeding and inoculation via water mass transport is an important vector connecting spatially separated habitats (Wilkins et al. 2013).

Conclusion

Spatiotemporal changes in MOx activity and MOB community structure in the water column above CH_4 seeps at the shallow shelf west of Svalbard are primarily a consequence of the seasonal variations of the hydrographical regimes. The two different scenarios presented in this study clearly show that seasonality strongly affects the MOB community structures and MOx capacity. Moreover, the distribution of MOB communities along the shallow shelf is most likely caused by physical transport, while site-specific geomorphological characteristics such as the shallow Forlandet moraine complex featuring numerous bathymetric depressions, enhance this effect. We suggest that the origin of the initial MOB "inoculum" in the bathymetric depressions offshore Prins Karls Forland might originate from seep regions further south. Once the MOB are trapped in bathymetric depressions, they are more sheltered from rapidly changing and dynamic conditions of the upper water column. Such sheltered conditions promote community growth, which in turn results in elevated MOx in summertime. Seasonality (especially in winter and spring, when the water column is subjected to deep mixing) is profoundly under-represented in studies on microbial habitat structure in Arctic water column habitats. Systematic time-series measurements covering the different, including harsh/bad weather seasons, would allow for a more comprehensive understanding of biogeochemical processes influenced by seasonal change-related microbial community variations. This would further improve our qualitative and quantitative understanding of important microbial processes in a warming Arctic Ocean.

References

Aagaard, K., A. Foldvik, and S. R. Hillman. 1987. The West Spitsbergen current: Disposition and water mass transformation. J. Geophys. Res. Oceans **92**: 3778–3784.

Allen, H. K., et al. 2016. Pipeline for amplifying and analyzing amplicons of the V1–V3 region of the 16S rRNA gene. BMC. Res. Notes **9**: 380.

Bergmann, G. T., and others. 2011. The under-recognized dominance of Verrucomicrobia in soil bacterial communities. Soil Biol. Biochem. **43**: 1450–1455.

Berndt, C., and others. 2014. Temporal constraints on hydrate-controlled methane seepage off Svalbard. Science **343**: 284–287.

Bushnell, B., J. Rood, and E. Singer. 2017. BBMerge – Accurate paired shotgun read merging via overlap. PLOS ONE **12**: e0185056. https://doi.org/10.1371/journal.pone.0185056

Bussmann, I. 2013. Distribution of methane in the Lena Delta and Buor-Khaya Bay, Russia. Biogeosciences **10**: 4641–4652.

Caporaso, J. G., and others. 2010. QIIME allows analysis of high-throughput community sequencing data. Nat. Methods **7**: 335–336.

Cottier, F., V. Tverberg, M. Inall, H. Svendsen, F. Nilsen, and C. Griffiths. 2005. Water mass modification in an Arctic fjord through cross-shelf exchange: The seasonal hydrography of Kongsfjorden, Svalbard. J. Geophys. Res. **110**: (C12005). doi:10.1029/2004JC002757

Cottier F. R., Nilsen F., Inall M. E., Gerland S., Tverberg V., Svendsen H. 2007. Wintertime warming of an Arctic shelf in response to large-scale atmospheric circulation. Geophysical Research Letters **34**: 1–5. doi:10.1029/2007GL029948

Crespo-Medina, M., and others. 2014. The rise and fall of methanotrophy following a deepwater oil-well blowout. Nat. Geosci. **7**: 423–427.

Damm, E., A. Mackensen, G. Budéus, E. Faber, and C. Hanfland. 2005. Pathways of methane in seawater: Plume spreading in an Arctic shelf environment (SW-Spitsbergen). Cont. Shelf Res. **25**: 1453–1472.

Dunfield, P. F., and others. 2007. Methane oxidation by an extremely acidophilic bacterium of the phylum Verrucomicrobia. Nature **450**: 879–882.

Edgar, R. C. 2004. MUSCLE: Multiple sequence alignment with high accuracy and high throughput. Nucleic Acids Res. **32**: 1792–1797.

Edgar, R. C. 2010. Search and clustering orders of magnitude faster than BLAST. Bioinformatics **26**: 2460–2461.

Edgar, R. C., B. J. Haas, J. C. Clemente, C. Quince, and R. Knight. 2011. UCHIME improves sensitivity and speed of chimera detection. Bioinformatics **27**: 2194–2200.

Etminan, M., G. Myhre, E. J. Highwood, and K. P. Shine. 2016. Radiative forcing of carbon dioxide, methane, and nitrous oxide: A significant revision of the methane radiative forcing. Geophys. Res. Lett. **43**: 12,614–612,623.

Ferré, B., and others. 2020. Reduced methane seepage from Arctic sediments during cold bottom-water conditions. Nat. Geosci. **13**: 144–148.

Freitas, S., and others. 2012. Global distribution and diversity of marine Verrucomicrobia. ISME J. **6**: 1499–1505.

Gentz, T., E. Damm, J. Schneider von Deimling, S. Mau, D. F. McGinnis, and M. Schlüter. 2014. A water column study of methane around gas flares located at the West Spitsbergen continental margin. Cont. Shelf Res. **72**: 107–118.

Giovannoni, S. J., and U. Stingl. 2005. Molecular diversity and ecology of microbial plankton. Nature **437**: 343–348.

Graves, C. A., and others. 2015. Fluxes and fate of dissolved methane released at the seafloor at the landward limit of the gas hydrate stability zone offshore western Svalbard. J. Geophys. Res. Oceans **120**: 6185–6201.

Graves, C. A., and others. 2017. Methane in shallow subsurface sediments at the landward limit of the gas hydrate stability zone offshore western Svalbard. Geochim. Cosmochim. Acta **198**: 419–438.

Hansen, J., M. Sato, G. Russell, and P. Kharecha. 2013. Climate sensitivity, sea level and atmospheric carbon dioxide. Philos. Trans. R. Soc. A: Math. Phys. Eng. Sci. **371**: 20120294. http://dx.doi.org/10.1098/rsta.2012.0294

Hansman, R. L., A. R. Thurber, L. A. Levin, and L. I. Aluwihare. 2017. Methane fates in the benthos and water column at cold seep sites along the continental margin of Central and North America. Deep-Sea Res. I Oceanogr. Res. Pap. **120**: 122–131.

Hanson, R. S., and T. E. Hanson. 1996. Methanotrophic bacteria. Microbiol. Rev. **60**: 439–471.

Heeschen, K. U., A. M. Tréhu, R. W. Collier, E. Suess, and G. Rehder. 2003. Distribution and height of methane bubble plumes on the Cascadia Margin characterized by acoustic imaging. Geol. Res. Lett. **30**: 1463.

Heijs, S. K., J. S. Sinninghe Damsté, and L. J. Forney. 2005. Characterization of a deep-sea microbial mat from an active cold seep at the Milano mud volcano in the Eastern Mediterranean Sea. FEMS Microbiol. Ecol. **54**: 47–56.

Herlemann, D. P. R., M. Labrenz, K. Jürgens, S. Bertilsson, J. J. Waniek, and A. F. Andersson. 2011. Transitions in bacterial communities along the 2000 km salinity gradient of the Baltic Sea. ISME J. **5**: 1571–1579.

James, R. H., and others. 2016. Effects of climate change on methane emissions from seafloor sediments in the Arctic Ocean: A review. Limnol. Oceanogr. **61**: S283–S299.

Knief, C. 2015. Diversity and habitat preferences of cultivated and uncultivated aerobic methanotrophic bacteria evaluated based on pmoA as molecular marker. Front. Microbiol. **6**: 1346.

Kozich, J. J., S. L. Westcott, N. T. Baxter, S. K. Highlander, and P. D. Schloss. 2013. Development of a dual-index sequencing strategy and curation pipeline for analyzing amplicon sequence data on the MiSeq illumina sequencing platform. Appl. Environ. Microbiol. **79**: 5112–5120.

Kruse, T., C. M. Ratnadevi, H.-A. Erikstad, and N.-K. Birkeland. 2019. Complete genome sequence analysis of the thermoacidophilic verrucomicrobial methanotroph "*Candidatus Methylacidiphilum kamchatkense*" strain Kam1 and comparison with its closest relatives. BMC Genomics **20**: 642.

Landvik, J. Y., and others. 2005. Rethinking late Weichselian ice-sheet dynamics in coastal NW Svalbard. Boreas **34**: 7–24.

Letunic, I., and P. Bork. 2016. Interactive tree of life (iTOL) v3: An online tool for the display and annotation of phylogenetic and other trees. Nucleic Acids Res. **44**: W242–W245.

Lozupone, C., M. E. Lladser, D. Knights, J. Stombaugh, and R. Knight. 2011. UniFrac: An effective distance metric for microbial community comparison. ISME J. **5**: 169–172.

Lüke, C., and P. Frenzel. 2011. Potential of pmoA amplicon pyrosequencing for methanotroph diversity studies. Appl. Environ. Microbiol. **77**: 6305–6309.

Masson-Delmotte, V., and others. 2006. Past and future polar amplification of climate change: Climate model

intercomparisons and ice-core constraints. Climate Dynam. **26**: 513–529.

Mau, S., and others. 2017. Widespread methane seepage along the continental margin off Svalbard - From Bjørnøya to Kongsfjorden. Sci. Rep. **7**: 42997.

Mau, S., J. Blees, E. Helmke, H. Niemann, and E. Damm. 2013. Vertical distribution of methane oxidation and methanotrophic response to elevated methane concentrations in stratified waters of the Arctic fjord Storfjorden (Svalbard, Norway). Biogeosciences **10**: 6267–6278.

Moussard, H., N. Stralis-Pavese, L. Bodrossy, J. D. Neufeld, and J. C. Murrell. 2009. Identification of active methylotrophic bacteria inhabiting surface sediment of a marine estuary. Environ. Microbiol. Rep. **1**: 424–433.

Murrell, J. C. 2010. The aerobic methane oxidizing bacteria (Methanotrophs). *In* K. N. Timmis [ed.], Handbook of hydrocarbon and lipid microbiology. Berlin Heidelberg: Springer-Verlag.

Myhre, C. L., and others. 2016. Extensive release of methane from Arctic seabed west of Svalbard during summer 2014 does not influence the atmosphere. Geophys. Res. Lett. **43**: 4624–4631.

Neufeld, J. D., H. Schäfer, M. J. Cox, R. Boden, I. R. McDonald, and J. C. Murrell. 2007. Stable-isotope probing implicates Methylophaga spp and novel Gammaproteobacteria in marine methanol and methylamine metabolism. ISME J. **1**: 480–491.

Neufeld, J. D., R. Boden, H. Moussard, H. Schäfer, and J. C. Murrell. 2008. Substrate-specific clades of active marine methylotrophs associated with a phytoplankton bloom in a temperate coastal environment. Appl. Environ. Microbiol. **74**: 7321–7328.

Niemann, H., and others. 2015. Toxic effects of lab-grade butyl rubber stoppers on aerobic methane oxidation. Limnol. Oceanogr.: Methods **13**: 40–52.

Nilsen, F., F. Cottier, R. Skogseth, and S. Mattsson. 2008. Fjord–shelf exchanges controlled by ice and brine production: The interannual variation of Atlantic Water in Isfjorden, Svalbard. Cont. Shelf Res. **28**: 1838–1853.

Nilsen, F., R. Skogseth, J. Vaardal-Lunde, and M. Inall. 2016. A simple shelf circulation model: Intrusion of Atlantic Water on the West Spitsbergen Shelf. J. Phys. Oceanogr. **46**: 1209–1230.

Op den Camp, H. J. M., and others. 2009. Environmental, genomic and taxonomic perspectives on methanotrophic Verrucomicrobia. Environ. Microbiol. Rep. **1**: 293–306.

Osudar, R., S. Liebner, M. Alawi, S. Yang, I. Bussmann, and D. Wagner. 2016. Methane turnover and methanotrophic communities in arctic aquatic ecosystems of the Lena Delta, Northeast Siberia. FEMS Microbiol. Ecol. **92**: fiw116. https://doi.org/10.1093/femsec/fiw116

Pilloni, G., M. S. Granitsiotis, M. Engel, and T. Lueders. 2012. Testing the limits of 454 pyrotag sequencing: Reproducibility, quantitative assessment and comparison to T-RFLP fingerprinting of aquifer microbes. PLoS One **7**: e40467.

Pol, A., K. Heijmans, H. R. Harhangi, D. Tedesco, M. S. M. Jetten, and H. J. M. Op den Camp. 2007. Methanotrophy below pH 1 by a new Verrucomicrobia species. Nature **450**: 874–878.

Portnov, A., S. Vadakkepuliyambatta, J. Mienert, and A. Hubbard. 2016. Ice-sheet-driven methane storage and release in the Arctic. Nat. Commun. **7**: 10314.

Quast, C., and others. 2013. The SILVA ribosomal RNA gene database project: Improved data processing and web-based tools. Nucleic Acids Res. **41**: D590–D596.

Redmond, M. C., D. L. Valentine, and A. L. Sessions. 2010. Identification of novel methane-, ethane-, and propane-oxidizing bacteria at marine hydrocarbon seeps by stable isotope probing. Appl. Environ. Microbiol. **76**: 6412–6422.

Reeburgh, W. S. 2007. Oceanic methane biogeochemistry. Am. Chem. Soc. **107**: 486–513.

Rehder, G., R. S. Keir, E. Suess, and M. Rhein. 1999. Methane in the northern Atlantic controlled by microbial oxidation and atmospheric history. Geophys. Res. Lett. **26**: 587–590.

Rognes, T., T. Flouri, B. Nichols, C. Quince, and F. Mahé. 2016. VSEARCH: A versatile open source tool for metagenomics. PeerJ **4**: e2584.

Sahling, H., and others. 2014. Gas emissions at the continental margin west off Svalbard: Mapping, sampling, and quantification. Biogeosci. Discuss. **11**: 7189–7234.

Sarkar, S., and others. 2012. Seismic evidence for shallow gas-escape features associated with a retreating gas hydrate zone offshore West Svalbard. J. Geophys. Res.-Solid Earth **117**: 1–18. doi:10.1029/2011JB009126

Schloss, P. D., and others. 2009. Introducing mothur: Open-source, platform-independent, community-supported software for describing and comparing microbial communities. Appl. Environ. Microbiol. **75**: 7537–7541.

Shakhova, N., I. Semiletov, A. Salyuk, V. Yusupov, D. Kosmach, and Ö. Gustafsson. 2010. Extensive methane venting to the atmosphere from sediments of the east Siberian Arctic shelf. Science **327**: 1246–1250.

Silyakova, A., and others. 2020. Physical controls of dynamics of methane venting from a shallow seep area west of Svalbard. Cont. Shelf Res. **194**: 104030.

Stamatakis, A. 2014. RAxML version 8: A tool for phylogenetic analysis and post-analysis of large phylogenies. Bioinformatics **30**: 1312–1313.

Steinle, L., and others. 2015. Water column methanotrophy controlled by a rapid oceanographic switch. Nat. Geosci. **8**: 378–382.

Steinle, L., and others. 2017. Effects of low oxygen concentrations on aerobic methane oxidation in seasonally hypoxic coastal waters. Biogeosciences **14**: 1631–1645.

Tavormina, P. L., and others. 2015. *Methyloprofundus sedimenti* gen. nov., sp. nov., an obligate methanotroph from ocean sediment belonging to the 'deep sea-1' clade of marine methanotrophs. Int. J. Syst. Evol. Microbiol. **65**: 251–259.

Tavormina, P. L., W. Ussler, and V. J. Orphan. 2008. Planktonic and sediment-associated aerobic methanotrophs in

two seep systems along the North American margin. Appl. Environ. Microbiol. **74**: 3985–3995.

Valentine, D. L., D. C. Blanton, W. S. Reeburgh, and M. Kastner. 2001. Water column methane oxidation adjacent to an area of active hydrate dissociation, Eel River Basin. Geochim. Cosmochim. Acta **65**: 2633–2640.

van Teeseling, M. C. F., and others. 2014. Expanding the verrucomicrobial methanotrophic world: Description of three novel species of Methylacidimicrobium gen. nov. Appl. Environ. Microbiol. **80**: 6782–6791.

von Appen, W. J., U. Schauer, T. Hattermann, and A. Beszczynska-Möller. 2016. Seasonal cycle of mesoscale instability of the West Spitsbergen current. J. Phys. Oceanogr. **46**: 1231–1254.

Wen, X., S. Yang, and S. Liebner. 2016. Evaluation and update of cutoff values for methanotrophic pmoA gene sequences. Arch. Microbiol. **198**: 629–636.

Westbrook, G. K., and others. 2009. Escape of methane gas from the seabed along the West Spitsbergen continental margin. Geophys. Res. Lett. **36**: 1–5.

Wiesenburg, D. A., and N. L. Guinasso. 1979. Equilibrium solubilities of methane, carbon monoxide, and hydrogen in water and sea water. J. Chem. Eng. Data **24**: 356–360.

Wilkins, D., E. van Sebille, S. R. Rintoul, F. M. Lauro, and R. Cavicchioli. 2013. Advection shapes Southern Ocean microbial assemblages independent of distance and environment effects. Nat. Commun. **4**: 2457.

Yarza, P., and others. 2014. Uniting the classification of cultured and uncultured bacteria and archaea using 16S rRNA gene sequences. Nat. Rev. Microbiol. **12**: 635–645.

Zhang, C., and others. 2017. Luteolibacter flavescens sp. nov., isolated from deep seawater. Int. J. Syst. Evol. Microbiol. **67**: 729–735.

Acknowledgments

We would like to thank the captain, crew, and scientific research party of the R/V *Helmer Hanssen* as well as the chief scientists of the cruises: CAGE15-3, CAGE16-4, CAGE16-5, and CAGE17-1. We are particularly grateful to the participants at BareLab, the Russian Scientific Center on Spitsbergen, and Anna Nikulina from the Arctic and Antarctic Research Institute (AARI) for their unelaborated and kind provision of laboratory facilities at Barentsburg. Matteus Lindgren is thanked for measuring methane concentrations in CAGE17-1 samples, JoLynn Carroll for her assistance in initiating the project, and Greta Reintjes for support in statistical analysis. Computations were performed using resources provided by UNINETT Sigma2—the National Infrastructure for High Performance Computing and Data Storage in Norway, account numbers NN9639K and NS9593K. This study is funded by CAGE (Centre for Arctic Gas Hydrate, Environment and Climate), Norwegian Research Council grant no. 223259.

Conflict of Interest

None declared.

Submitted 14 July 2020
Revised 29 November 2020
Accepted 01 March 2021

Associate editor: Lauren Juranek